

Long-Jun Dai, Hyung Sub Kang, Dirk Kerstan, Gordon Ritchie and Gary A. Quamme

Am J Physiol Renal Physiol 281:833-840, 2001. First published Jul 12, 2001;
doi:10.1152/ajprenal.0349.2000

You might find this additional information useful...

This article cites 28 articles, 21 of which you can access free at:

<http://ajprenal.physiology.org/cgi/content/full/281/5/F833#BIBL>

This article has been cited by 3 other HighWire hosted articles:

Purinergic Signaling Along the Renal Tubule: The Current State of Play

R. J. Unwin, M. A. Bailey and G. Burnstock
Physiology, December 1, 2003; 18 (6): 237-241.
[\[Abstract\]](#) [\[Full Text\]](#) [\[PDF\]](#)

Molecular Physiology of P2X Receptors

R. A. North
Physiol Rev, October 1, 2002; 82 (4): 1013-1067.
[\[Abstract\]](#) [\[Full Text\]](#) [\[PDF\]](#)

Adenosine modulates Mg²⁺ uptake in distal convoluted tubule cells via A1 and A2 purinoceptors

H. S. Kang, D. Kerstan, L.-J. Dai, G. Ritchie and G. A. Quamme
Am J Physiol Renal Physiol, December 1, 2001; 281 (6): F1141-F1147.
[\[Abstract\]](#) [\[Full Text\]](#) [\[PDF\]](#)

Updated information and services including high-resolution figures, can be found at:

<http://ajprenal.physiology.org/cgi/content/full/281/5/F833>

Additional material and information about *AJP - Renal Physiology* can be found at:

<http://www.the-aps.org/publications/ajprenal>

This information is current as of October 1, 2007 .

ATP inhibits Mg^{2+} uptake in MDCT cells via P2X purinoceptors

LONG-JUN DAI, HYUNG SUB KANG, DIRK KERSTAN,
GORDON RITCHIE, AND GARY A. QUAMME

Department of Medicine, University of British Columbia, Vancouver Hospital
and Health Sciences Centre, Vancouver, British Columbia, Canada V6T 1Z3

Received 21 December 2000; accepted in final form 18 June 2001

Dai, Long-Jun, Hyung Sub Kang, Dirk Kerstan, Gordon Ritchie, and Gary A. Quamme. ATP inhibits Mg^{2+} uptake in MDCT cells via P2X purinoceptors. *Am J Physiol Renal Physiol* 281: F833–F840, 2001. First published July 12, 2001; 10.1152/ajprenal.00349.2001.—Nucleotides have diverse effects on water and electrolyte reabsorption within the distal tubule of the nephron. As the distal tubule is important in control of renal Mg^{2+} balance, we determined the effects of ATP on cellular Mg^{2+} uptake in this segment. The effects of ATP on immortalized mouse distal convoluted tubule (MDCT) cells were studied by measuring Mg^{2+} uptake with fluorescence techniques. The mean basal Mg^{2+} uptake rate was 165 ± 6 nM/s. ATP inhibited basal Mg^{2+} uptake and hormone-stimulated Mg^{2+} entry by 40%. Both P2X (P2X1–P2X5 subtypes) and P2Y2 receptor subtypes were identified in MDCT cells using differential RT-PCR. Activation of both receptor subtypes with selective agonists increased intracellular Ca^{2+} concentration, P2X purinoceptors by ionotropic-gated channels, and P2Y receptors via G protein-mediated intracellular Ca^{2+} release. The more relatively selective P2X agonists [β,γ -methylene ATP (β,γ -Me-ATP) and 2'- and -3'-O-(4-benzoyl-benzoyl)-ATP] inhibited arginine vasopressin (AVP)- and parathyroid hormone (PTH)-mediated Mg^{2+} uptake whereas agonists more selective for P2Y purinoceptors (UTP, ADP, and 2-methylthio-ATP) were without effect. Removal of extracellular Ca^{2+} diminished β,γ -Me-ATP-mediated increase in intracellular Ca^{2+} and inhibition of AVP-stimulated Mg^{2+} entry. We conclude from this information that ATP inhibited Mg^{2+} uptake in MDCT cells through P2X purinoceptors expressed in this distal convoluted tubule cell line.

intracellular magnesium, fluorescence; adenosine triphosphate; P2Y purinoceptors; prostanoids; intracellular calcium transients; intracellular adenosine 3',5'-cyclic monophosphate; immortalized mouse distal convoluted tubule cells

EXTRACELLULAR NUCLEOTIDES have important effects on water and electrolyte transport in the distal tubule of the kidney (3, 18). Extracellular ATP inhibits arginine vasopressin (AVP)-stimulated water transport in rabbit cortical collecting ducts (CCD) and rat inner medullary collecting ducts (IMCD) and sodium absorption in CCD and medullary collecting duct cells (13, 15, 22).

Nucleotides activate K^+ channels and stimulate Cl^- secretion in Madin-Darby canine kidney (MDCK) cells and *Xenopus laevis* renal (A6) cells, which are models for distal tubular function (12, 23). Nucleotides also regulate NaCl transport in IMCD, the final nephron segment responsible for fine adjustments in NaCl excretion (17). Extracellular ATP has also been reported to inhibit Ca^{2+} absorption in a mixture of isolated rabbit cortical connecting tubules and CCD cells (15, 26). Accordingly, purinoceptor agonists play an important role in determining water and electrolyte reabsorption in the final segments of the nephron. Unlike sodium and Ca^{2+} , the terminal segments involved with tubular Mg^{2+} reabsorption comprise only the convoluted portion of the distal tubule. The distal convoluted tubule reabsorbs $\sim 15\%$ of the filtered Mg^{2+} or 90% of the Mg^{2+} delivered to it from the loop of Henle (20). As there is no Mg^{2+} reabsorbed beyond this segment, the distal tubule acts as the final control in determining the final urinary excretion. Accordingly, characterization of the effects of purinergic nucleotides on Mg^{2+} uptake in distal convoluted tubule cells would be important to understanding its role in overall renal Mg^{2+} handling.

Extracellular ATP acts through P2 purinoceptors, which have been divided into P2X and P2Y receptor families (1). The P2X receptor family contains a least seven distinct subtypes, all of which are ATP-gated ion channels that on activation form Ca^{2+} -permeable channels permitting extracellular Ca^{2+} entry into the intracellular fluid (21). P2X agonists include α,β -methylene-ATP (α,β -Me-ATP) and the more selective β,γ -methylene-ATP (β,γ -Me-ATP) and [2'- and -3'-O-(4-benzoyl-benzoyl)-ATP] (benzoyl-benzoyl-ATP). The P2Y receptors, comprising at least six subtypes, are widely expressed and differ in their specificity for nucleotides. P2Y1 receptors bind ATP and the synthetic agonist α,β -Me-ATP whereas P2Y2 receptors respond to both ATP and UTP (21). P2Y receptors are coupled to G proteins that increase the activity of phospholipase C, D, and A_2 , release intracellular Ca^{2+} , and activate protein kinase C (21). P2Y receptors may also stimu-

Address for reprint requests and other correspondence: G. A. Quamme, Dept. of Medicine, Vancouver Hospital and Health Sciences Centre, Koerner Pavilion, 2211 Wesbrook Mall, Vancouver, BC Canada, V6T 1Z3 (E-mail:quamme@interchange.ubc.ca).

The costs of publication of this article were defrayed in part by the payment of page charges. The article must therefore be hereby marked "advertisement" in accordance with 18 U.S.C. Section 1734 solely to indicate this fact.

late or inhibit adenylate cyclase depending on the cell type (21). In those cells in which adenylate cyclase is stimulated, the increase in intracellular cAMP production is sensitive to indomethacin, suggesting that cyclooxygenase-derived products mediate this response (17, 19). Additionally, ATP can be metabolized by ecto-ATPases to adenosine, the natural agonist for adenosine, or P1 receptors, all of which couple to G proteins (21). We have shown that hormone receptor-mediated intracellular cAMP formation, stimulation of protein kinase A and phospholipase C, or protein kinase C activation importantly affects Mg^{2+} entry in mouse DCT (MDCT) cells (5, 7). As ATP might act through these intracellular pathways, we determined the effect of purinergic nucleotides on hormone-stimulated Mg^{2+} uptake in distal tubule cells.

In the present studies, we determined the effect of ATP on Mg^{2+} uptake in immortalized MDCT cells (11). The MDCT cell line possesses many of the properties of the intact distal convoluted tubule. Parathyroid hormone (PTH) and calcitonin stimulate Ca^{2+} and Mg^{2+} uptake whereas glucagon and AVP increase Mg^{2+} entry in MDCT cells (5, 7, 11). The distal convoluted tubule has not been extensively studied because it is difficult to perform in vitro perfusion experiments, so we used this cell line as a model to investigate the actions of ATP on Mg^{2+} uptake in this segment. Mg^{2+} uptake rate, measured with microfluorescence using mag-fura, is concentration dependent and selective for Mg^{2+} (8). Moreover, the influx rate is rapid and reproducible so that it is possible to determine the effects of extracellular influences on transport rates. In the present study, we show that ATP inhibits basal and hormone-stimulated Mg^{2+} entry in MDCT cells via P2X purinoceptors.

MATERIALS AND METHODS

Cell culture. Distal convoluted tubule cells were isolated from mice, immortalized, and functionally characterized as previously described by Friedman and Gesek et al. (11). The MDCT cell line was grown on 60-mm plastic culture dishes (Corning Glass Works, Corning Medical and Scientific, Corning, NY) in basal DMEM/Ham's-F-12, 1:1, media (GIBCO) supplemented with 10% FCS (Flow Laboratories, McLean, VA.), 1 mM glucose, 5 mM L-glutamine, 50 U/ml penicillin, and 50 μ g/ml streptomycin in a humidified environment of 5% CO_2 -95% air at 37°C. For the fluorescence studies, confluent cells were washed three times with PBS containing 5 mM EGTA, trypsinized, and seeded on glass coverslips. Aliquots of harvested cells were allowed to settle onto sterile glass coverslips in 100-mm Corning tissue culture dishes, and the cells were grown to subconfluence over 1–2 days in supplemented media as described above. The normal media contained 0.6 mM Mg^{2+} and 1.0 mM Ca^{2+} . In the experiments indicated, MDCT cells were cultured in Mg^{2+} -free media (<0.01 mM) where indicated for 16–24 h before study. Other constituents of the Mg^{2+} -free culture media were similar to those of the complete media. Customized Mg^{2+} -free media were purchased from Stem Cell Technologies (Vancouver, BC). These media contained 0.2% BSA rather than FCS.

Determination of cAMP concentration. cAMP was determined in confluent MDCT cell monolayers cultured in 24-well plates in DMEM-Ham's F-12 media without serum but

with 0.1% BSA. The media contained 0.6 mM Mg^{2+} or zero Mg^{2+} where indicated. After addition of either PTH or AVP, MDCT cells were incubated at 37°C for 5 min in the presence of 0.1 mM IBMX. The hormones were obtained from Sigma. The cAMP was extracted with 5% trichloroacetic acid that was removed with ether, and the extract was acidified with 0.1 N HCl. The aqueous phase was dried and then dissolved in Tris-EDTA buffer, and cAMP was measured with a radioimmunoassay kit (Diagnostic Products, Los Angeles, CA).

Cytoplasmic Mg^{2+} and Ca^{2+} measurements. Coverslips were mounted into a perfusion chamber, and intracellular Mg^{2+} concentration ($[Mg^{2+}]_i$) and intracellular Ca^{2+} concentrations ($[Ca^{2+}]_i$) were determined with the use of the Mg^{2+} -sensitive and Ca^{2+} -sensitive fluorescent dyes mag-fura 2 and fura 2, respectively (Molecular Probes, Eugene, OR). The cell-permeant acetoxymethyl ester form of the dye was dissolved in DMSO to a stock concentration of 5 mM and then diluted to 5 μ M mag-fura 2-AM or 10 μ M fura 2-AM in media for 20 min at 37°C. Cells were subsequently washed three times with buffered salt solution containing (in mM) 145 NaCl, 4.0 KCl, 0.8 Na_2HPO_4 , 0.2 KH_2PO_4 , 1.0 $CaCl_2$, 5 glucose, and 20 HEPES-Tris, at pH 7.4. The MDCT cells were incubated for a further 20 min to allow for complete deesterification and washed once before measurement of fluorescence.

Epifluorescence microscopy was used to monitor changes in the mag-fura 2 or fura 2 fluorescence of the MDCT cell monolayer. The chamber was mounted on an inverted Nikon Diaphot-TMD microscope with a Fluor $\times 100$ objective, and fluorescence was monitored under oil immersion within a single cell over the course of study. Fluorescence was recorded at 1-s intervals using a dual-excitation wavelength spectrofluorometer (Delta-scan, Photon Technologies, Princeton, NJ) with excitation for mag-fura 2 at 335 and 385 nm, for fura 2 at 340 and 380 nm (chopper speed set at 100 Hz/s), and for emission at 505 nm. Media changes were made without an interruption in recording.

The free $[Mg^{2+}]_i$ and $[Ca^{2+}]_i$ were calculated from the ratio of the fluorescence at the two excitation wavelengths as described, using a dissociation constant (K_d) of 1.4 mM and 224 nM, respectively, for the mag-fura 2- Mg^{2+} and fura 2- Ca^{2+} complexes (5). The minimum (R_{min}) and maximum (R_{max}) ratios were determined for the cells at the end of each experiment using 20 μ M digitonin. R_{max} for mag-fura 2 was found by the addition of 50 mM $MgCl_2$ in the absence of Ca^{2+} , and R_{min} was obtained by removal of Mg^{2+} and addition of 100.0 mM EDTA, pH 7.2. The excitation spectrum of the cellular mag-fura 2 under these conditions was similar to that of free mag-fura 2 in the same solutions. R_{max} and R_{min} for fura 2 were obtained with Ca^{2+} and EGTA by previously published techniques (5).

RT-PCR analysis and differential DNA sequencing. Total RNA was extracted from confluent MDCT cells using TRIzol reagent (GIBCO BRL) according to the manufacturer's instructions. Briefly, cells from a 150-cm² flask were rinsed in 5 ml PBS, pelleted, and lysed with a 5-min incubation in 2 ml TRIzol reagent. The mixture was shaken vigorously for 60 s after 0.4 ml chloroform was added. The mixture was centrifuged at 14,000 g for 15 min, and the upper aqueous phase containing the extracted RNA was aspirated. RNA was precipitated from the aqueous phase by an equal volume of isopropanol and pelleted with centrifugation at 14,000 g for 15 min at 4°C. The RNA precipitate was washed two times with 75% ice-cold ethanol, dried, and taken up in 200 μ l diethylpyrocarbonate-treated distilled H₂O. Ten micrograms of RNA were incubated with RNase-free DNase (134 U) in the presence of 5 mM $MgCl_2$ at 37°C for 10 min. The DNase

was heat inactivated with a 5-min incubation at 99°C, and the product was stored at -80°C. The same procedure was used to prepare total RNA from mouse cortical kidney.

RT-PCR was carried out as follows. Total RNA (5 µg) was reverse-transcribed with the use of Superscript II RT from (GIBCO BRL Life Technologies). One microliter of cDNA was used for PCR amplification. We used degenerate primers for rat P2X1, P2X2, and P2X3 receptors as described by Filipovic et al. (10) and McCoy et al. (17). The forward primer was 5'-TTC ACC (C/A/T/T/C) (T/C)TC ATC AA(G/A) AAC AGC ATC-3', and the reverse primer was 5'-TGG CAA A(C/T)C TGA AGT TG(A/T) AGC C-3'. The PCR reaction (total volume 50 µl) consisted of 32 cycles at 94°C for 30 s, annealing at 52°C for 30 s, and polymerization at 72°C for 30 s using a GeneAmp PCR system thermocycler (model 2400, Perkin-Elmer, Branchburg, NJ). The PCR products were extracted from agarose gels and ligated into pGem-T Easy Vector systems (Promega). Ligations were transfected into DH5 α -competent cells, and successful insertions were selected from colonies grown on LB-agar plates. Specific primers were designed from mouse sequences to amplify P2X4–P2X7 receptors. The primers were for the following: P2X4, forward primer, 5'-GAG AAT GAC GCT GGT GTG CC-3'; reverse primer, 5'-TTG GTG AGT GTG CGT TGC TC-3'; for P2X5, forward primer, 5'-TCC ACC AAT CTC TAC TGC-3'; reverse primer, 5'-CCA GGT CAC AGA AGA AAG-3'; for P2X6, forward primer, 5'-TAC GTA CTA ACA GAC GCA-3'; reverse primer, 5'-ATA TCA GGG TTC TTT GGG-3'; and for P2X7, forward primer, 5'-AAG TCT CTG CCT GGT GTC-3', and reverse primer, 5'-GGC ATA TCT GAA GTT GTA GC-3'. The primers for P2Y2 mRNA comprised 5'-CGT CAT CCT TGT CTG TTA CGT GCT-3' and 5'-CTA CAG CCG AAT GTC CTT AGT G-3' (17). The PCR reaction for P2X4/P2X5 consisted of 35 cycles at 94°C for 30 s, annealing at 62°C for 30 s, and polymerization at 72°C for 30 s and for P2X6/P2X7 consisted of 35 cycles at 94°C for 30 s, annealing at 50°C for 30 s, and polymerization at 72°C for 30 s. Aliquots (8 µl) of the PCR reaction were electrophoresed through ethidium bromide-stained 1% agarose gels run with a 100-bp DNA ladder. The PCR products were extracted from agarose gels by established techniques and sequenced by Amplicon Express (Pullman, WA). The DNA sequence was screened with the basic local alignment search tool algorithm to compare with known P2X and P2Y2 receptor sequences.

Statistical analysis. Representative tracings of fluorescence intensities are given, and significance was determined by Student's *t*-test or Tukey's ANOVA as appropriate. A probability of $P < 0.05$ was taken to be statistically significant. All results are means \pm SE where indicated.

RESULTS

Extracellular ATP diminishes basal and prostaglandin-stimulated Mg^{2+} uptake into Mg^{2+} -depleted MDCT cells. Because there is not an appropriate radioisotope for Mg^{2+} to directly measure Mg^{2+} transport rates, we developed the following model to assess Mg^{2+} influx into single MDCT cells (7). Subconfluent MDCT monolayers were cultured in Mg^{2+} -free medium for 16 h. These cells possessed a significantly lower $[Mg^{2+}]_i$, 0.22 ± 0.01 mM, than that observed in normal MDCT cells, 0.53 ± 0.02 mM. When the Mg^{2+} -depleted MDCT cells were placed in a bathing solution containing 1.5 mM $MgCl_2$, the $[Mg^{2+}]_i$ increased with time and plateaued at 0.52 ± 0.06 mM, $n = 9$, which was similar to that observed for normal cells (7). The mean rate of

refill, $d([Mg^{2+}]_i)/dt$, measured as the change in $[Mg^{2+}]_i$ with time, was 165 ± 6 nM/s, $n = 6$ experiments, as determined over the first 500 s after the addition of Mg^{2+} . We have previously reported data that indicate the Mg^{2+} uptake is concentration dependent and selective for Mg^{2+} (8).

We determined the effect of ATP on basal and hormone-stimulated Mg^{2+} uptake in MDCT cells (Fig. 1). ATP (10^{-4} M) significantly inhibited the basal mean Mg^{2+} entry rate, 109 ± 4 nM/s, $n = 3$. We have reported that endogenously produced prostanoids stimulate Mg^{2+} uptake in MDCT cells so that the addition of indomethacin, a cyclooxygenase inhibitor, diminishes basal Mg^{2+} uptake (6). To test the idea that ATP may decrease basal Mg^{2+} uptake by inhibiting this auto-stimulatory pathway, we treated the MDCT cells with indomethacin and ATP. The percent inhibition was similar with indomethacin alone, 100 ± 20 nM/s, $n = 4$, as with indomethacin plus ATP, 83 ± 17 nM/s, $n = 5$ (Fig. 1). We have also shown that exogenously administered PGE_2 stimulates Mg^{2+} entry into MDCT cells by $49 \pm 9\%$ (6). Accordingly, we tested the effect of ATP on PGE_2 -mediated Mg^{2+} uptake. Pretreatment of cells with ATP diminishes PGE_2 -stimulated Mg^{2+} entry from 245 ± 23 nM/s, $n = 4$, to 89 ± 11 nM/s, $n = 3$ (Fig. 1). These studies suggest that ATP inhibits endogenously generated prostaglandins and exogenously applied PGE_2 . In those studies indicated, we performed

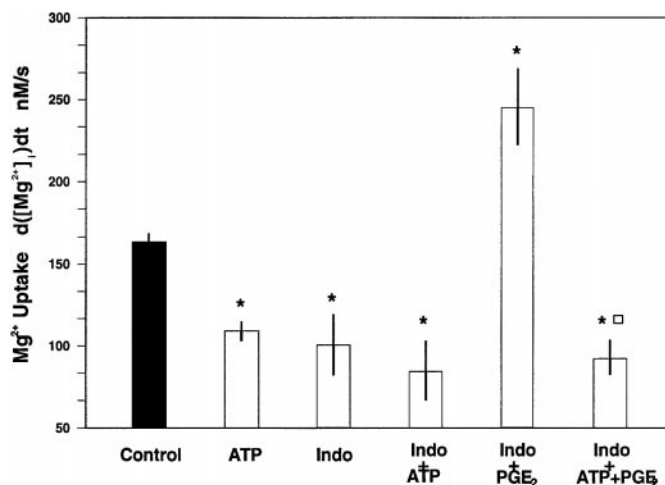


Fig. 1. ATP inhibits basal and prostaglandin-mediated Mg^{2+} uptake in Mg^{2+} -depleted mouse distal convoluted tubule (MDCT) cells. MDCT cells were cultured in Mg^{2+} -free media (<0.01 mM) for 16 h. Fluorescence studies were performed in buffer solutions in absence of external Mg^{2+} , and where indicated, $MgCl_2$ (1.5 mM final concentration) was added to observe changes in intracellular Mg^{2+} concentration ($[Mg^{2+}]_i$). The buffer solutions contained (in mM) 145 NaCl, 4.0 KCl, 0.8 K_2HPO_4 , 0.2 KH_2PO_4 , 1.0 $CaCl_2$, 5.0 glucose, and 10 HEPES-Tris, pH 7.4, with and without 1.5 mM $MgCl_2$. ATP, 10^{-4} M, was added to this buffer solution from a stock ethanol solution. Where indicated, MDCT cells were treated with 5 µM indomethacin (Indo) 15 min before experimentation according to the methods given in Ref. 4. PGE_2 was added from stock solutions at final concentrations of 10^{-7} M. Fluorescence was measured at 1 data point/s with 25-point signal averaging, and tracing was smoothed according to methods previously described (4). Values are means \pm SE for 3–7 cells. * $P < 0.01$, significance of Mg^{2+} entry rates compared with control values. □ Significance of ATP+ PGE_2 vs. ATP.

the experiments with indomethacin-treated cells to avoid the effects of autostimulation of prostaglandin formation.

ATP inhibits hormone-stimulated Mg^{2+} entry in MDCT cells. We have shown that PTH and AVP stimulate Mg^{2+} uptake into Mg^{2+} -depleted MDCT cells by 27 ± 4 and $21 \pm 5\%$, respectively, above basal entry rates (7, 8). Pretreatment of MDCT cells with ATP reduced PTH-stimulated Mg^{2+} uptake by $19 \pm 3\%$, $n = 5$ (Fig. 2). ATP diminished AVP-stimulated uptake from 201 ± 9 to 102 ± 8 nM/s, $n = 5$, which was similar to ATP-treated cells, 109 ± 4 nM/s, $n = 3$ (Fig. 2). The reason for these differences in inhibition of ATP on PTH and AVP is not known but may suggest differences in intracellular hormone receptor-mediated signaling pathways. As mentioned above, ATP inhibited PGE_2 -responsive Mg^{2+} influx to 89 ± 11 nM/s, $n = 3$, similar to that observed for ATP plus AVP.

MDCT cells possess P2X and P2Y purinoceptor subtypes. To characterize the purinogenic response, we determined both biochemical and functional expression of purinoceptors in MDCT cells. Expression of P2X receptor mRNA in MDCT cells was determined by RT-PCR using degenerate primers of P2X1–P2X3 and specific primers for each of P2X4–P2X7. As shown in Fig. 3, amplified PCR products of the expected size were identified for P2X1–P2X3 (500 bp). Twenty-seven colony picks were sequenced with the following results (number of positive picks given in brackets): P2X1 (1); P2X2 (10); and P2X3 (13). PCR products of the correct size were also observed for P2X4 and P2X5 in three separate PCR reactions using specific primers (Fig. 3). In addition, the MDCT cells possessed P2Y2 receptor mRNA (Fig. 3). The negative control (no cDNA) had no PCR products, and the positive control, cortical renal

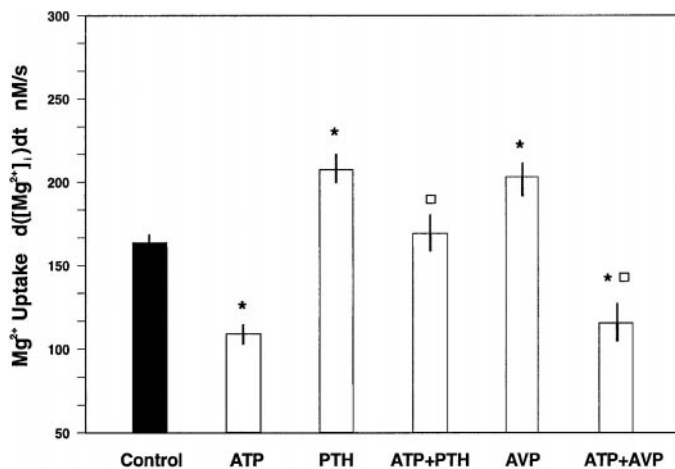


Fig. 2. ATP inhibits hormone-stimulated Mg^{2+} entry in MDCT cells. Where indicated parathyroid hormone (PTH), 10^{-7} M, or arginine vasopressin (AVP), 10^{-7} M, was added 5 min after ATP, 10^{-4} M, treatment. The rate of Mg^{2+} influx as determined by $d([Mg^{2+}]_i)/dt$ was measured using fluorescence techniques performed according to that given in legend to Fig. 1. $d([Mg^{2+}]_i)/dt$ values were determined over the first 500 s of fluorescence measurements. Values are means \pm SE for 3–6 cells. * $P < 0.01$, significance of Mg^{2+} entry rates compared with control values. □ Significance of ATP+PTH vs. PTH and ATP+AVP vs. AVP.

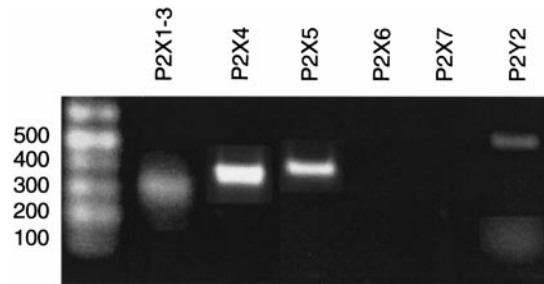


Fig. 3. RT-PCR analysis of P2X and P2Y2 purinoceptors in MDCT cells. Amplification of P2 receptors was performed using degenerate primers for P2X1–3 and specific primers for P2Y2 and P2X4–7 DNA fragments. Differential sequencing of the P2X1–P2X3 PCR products resulted in (positive colony picks in parentheses) P2X1 (1), P2X2 (10), and P2X3 (13). Renal cortical tissue was used as the positive control (not shown), and “no cDNA” was used as negative PCR control.

tissue, possessed a number of bands of the expected sizes (not shown). The identity of all RT-PCR products was verified by sequencing. The P2X and P2Y fragments identified in MDCT cells had the same sequence alignment reported for mouse cDNA. These results indicate that five members of the P2X receptor family and at least one member of the P2Y receptor family are represented in MDCT cells. Taylor et al. (25) reported a high incidence of multiple coexpression of P2X purinoceptor isoforms in a large number of different pulmonary- and gastrointestinal-derived epithelial cells. The most common isoforms were P2X2–P2X7, with P2X6 being noticeably absent from these cells (25). The observation that multiple subtypes are represented in the MDCT cell line used here is consonant with these findings in other epithelial cells.

Next, we determined whether the purinoceptors identified by PCR were functionally expressed in MDCT cells. Receptor-mediated intracellular Ca^{2+} signaling was assessed by fluorescence measurements using relatively selective agonists of the P2X and P2Y receptors. At present, there are no agonists or antagonists that discriminate adequately between the P2X and P2Y receptor families or between subtypes of receptors within each of these groups (21). Nevertheless, some of the most useful agonists are the stable ATP analogs α, β -Me-ATP and β, γ -Me-ATP that, if effective, strongly imply actions at P2X receptors and are generally inactive at P2Y receptors. ADP, UTP, UDP, and 2-methylthio ATP (2-MeS-ATP) are more selective for P2Y purinoceptors. All of the nucleotides tested resulted in transient increases in $[Ca^{2+}]_i$, but the concentration profiles were different (Table 1). ATP, ADP, UTP, and 2-MeS-ATP produced Ca^{2+} transients that were characterized by rapid basal-to-peak increases in Ca^{2+} concentration, in excess of 500 nM, which then rapidly subsided to a level that was 20–40 nM higher than basal concentrations for 5 min before returning to basal levels (Fig. 4, top). This profile is typical of receptor-mediated intracellular Ca^{2+} signaling characteristic of P2Y purinoceptors. The more selective P2X purinoceptor agonist, β, γ -Me-ATP, resulted in a relatively delayed increase in Ca^{2+} that did not attain the

Table 1. Purinoceptor agonists stimulate cytosolic Ca^{2+} transients in MDCT cells

Nucleotide	With Extracellular Ca^{2+}		Without Extracellular Ca^{2+}	
	Basal $[Ca^{2+}]_i$, nM	$\Delta[Ca^{2+}]_i$, nM	Basal $[Ca^{2+}]_i$, nM	$\Delta[Ca^{2+}]_i$, nM
ATP	87 ± 3 (6) ⁿ	$568 \pm 54^*$ (4)	92 ± 7 (3) ⁿ	$382 \pm 42^*$ (3)
ADP	90 ± 3 (3)	$517 \pm 190^*$ (3)		
UTP	90 ± 5 (3)	$1310 \pm 145^*$ (3)		
2MeS-ATP	84 ± 2 (4)	$205 \pm 99^*$ (3)	73 ± 3 (3) ⁿ	$347 \pm 128^*$ (3)
β,γ -Me-ATP	81 ± 3 (3)	$293 \pm 54^*$ (4)	73 ± 3 (3) ⁿ	$71 \pm 9^*$ (3)

Values are means \pm SE with the number of separate observations in parentheses. 2MeS-ATP, 2-methylthio-ATP; β,γ -Me-ATP, β,γ -methylene ATP. Normal mouse distal convoluted tubule (MDCT) cells were loaded with fura 2, and the purinoceptor agonists were added to buffer solutions at a concentration of 10^{-4} M. Intracellular Ca^{2+} concentration ($[Ca^{2+}]_i$) was measured with microfluorescence using fura 2. The change in intracellular Ca^{2+} concentration, ($\Delta[Ca^{2+}]_i$), was the maximal change in cytosolic Ca^{2+} from basal $[Ca^{2+}]_i$. $[Ca^{2+}]_i$ was measured with (1.0 mM extracellular calcium) and without (0 mM calcium, 0.5 mM EGTA). * $P < 0.001$ basal $[Ca^{2+}]_i$.

maximal levels observed with the other nucleotides used (Fig. 4, bottom). This was more characteristic of receptor-gated Ca^{2+} channels, as would be expected of P2X purinoceptors. In support of these conclusions, the

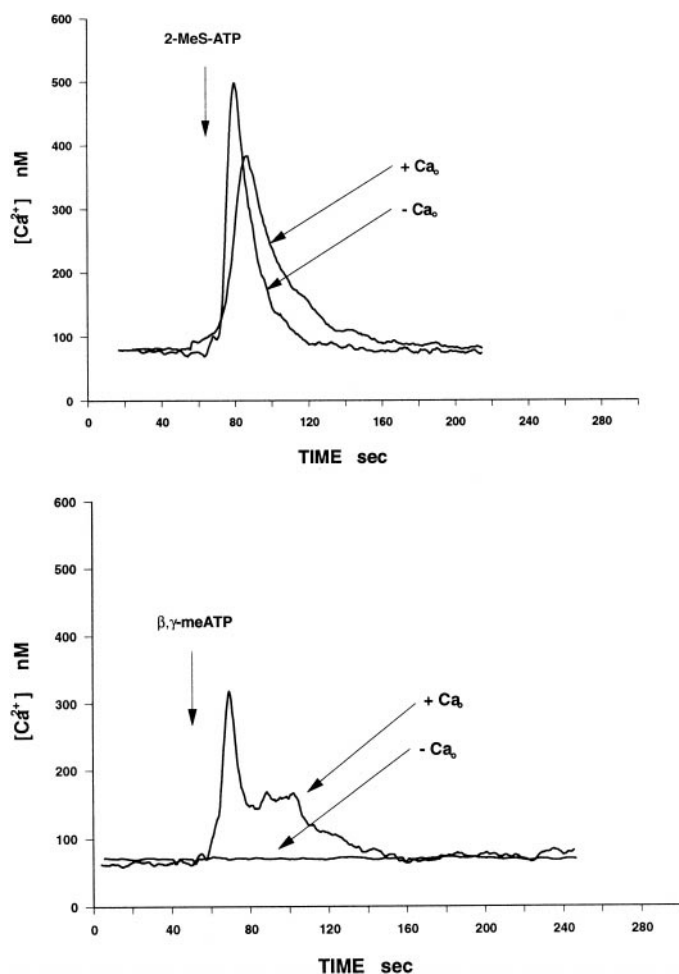
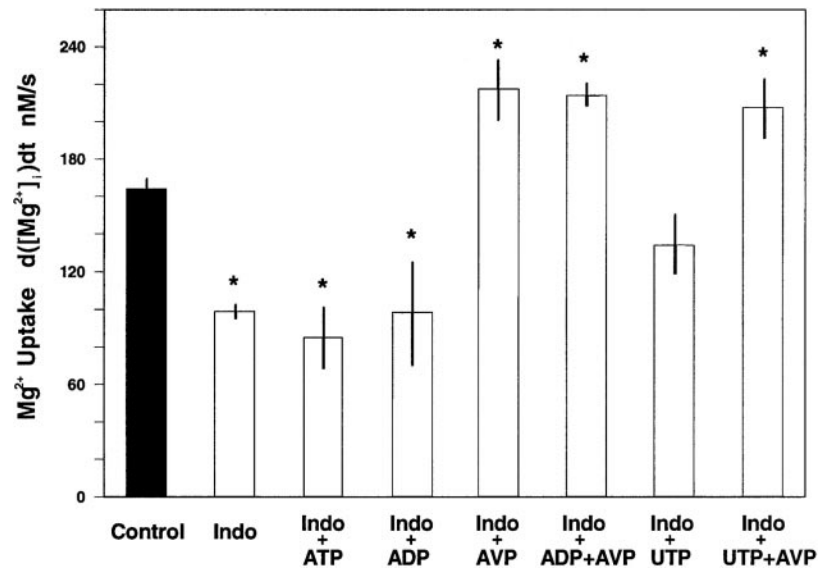


Fig. 4. Nucleotide-mediated Ca^{2+} signals in immortalized MDCT cells. The P2Y and P2X agonists 2-methylthio-ATP (2-MeS-ATP; top) and β,γ -methylene ATP (β,γ -Me-ATP; bottom) were added where indicated at concentrations of 10^{-4} M. Intracellular free Ca^{2+} concentration ($[Ca^{2+}]_i$) was determined by microfluorescence on single subconfluent MDCT cells using fura 2. Also shown is the effect of removal of the external Ca^{2+} (Ca_0^{2+}) from bath buffer solution with the addition of 0.5 mM EGTA. The mean Ca^{2+} values are given in Table 1.

increase in intracellular Ca^{2+} by β,γ -Me-ATP was abolished by removal of extracellular Ca^{2+} whereas the initial rapid Ca^{2+} transients of ATP, ADP, UTP, and 2-MeS-ATP remained evident after the removal of bath Ca^{2+} (Fig. 4 and Table 1). These biochemical and functional studies suggest that both P2Y and P2X receptor subtypes are represented in MDCT cells: activation of P2Y leads to receptor-mediated intracellular Ca^{2+} signaling and Ca^{2+} entry, and P2X results in increases in intracellular Ca^{2+} concentration via receptor-gated Ca^{2+} channels.

ATP inhibits hormone-mediated Mg^{2+} uptake through P2X purinoceptors. Next, we tested the effect of the selective nucleotides on AVP-stimulated Mg^{2+} uptake in MDCT cells. The addition of ADP, 99 ± 26 nM/s, $n = 3$, or UTP, 134 ± 16 nM/s, $n = 5$, did not change AVP-stimulated Mg^{2+} uptake, 214 ± 6 nM/s, $n = 3$ (Fig. 5). The more selective P2Y receptor agonist, 2-MeS-ATP, also did not change AVP-mediated Mg^{2+} entry rates, 234 ± 29 nM/s (Fig. 6). In these latter studies, the cells were not treated with indomethacin. The P2X agonist β,γ -Me-ATP, on the other hand, inhibited AVP-responsive Mg^{2+} entry, 79 ± 23 nM/s (Fig. 7). In support of the observation that P2X purinoceptor agonists inhibit hormone-stimulated Mg^{2+} entry, we showed that another P2X agonist, benzoyl-benzoyl-ATP, diminished PTH-stimulated Mg^{2+} uptake from 209 ± 8 nM/s, $n = 5$, to 89 ± 19 nM/s, $n = 4$. Accordingly, P2X purinoceptor-selective agonists inhibit hormone-stimulated Mg^{2+} entry in MDCT cells. It was of interest that P2Y receptor agonists increase intracellular Ca^{2+} release and Ca^{2+} entry through coupling to G proteins whereas P2X receptor agonists increase intracellular Ca^{2+} via receptor-gated Ca^{2+} entry. To evaluate the significance of extracellular Ca^{2+} entry in P2X purinoceptor responses, we performed studies in the absence of an extracellular Ca^{2+} that abolishes P2X receptor-mediated increases in $[Ca^{2+}]_i$ (Fig. 5). Removal of the extracellular Ca^{2+} and the addition of EGTA to the bathing solution prevented β,γ -Me-ATP inhibition of AVP-stimulated Mg^{2+} uptake, 270 ± 23 nM, $n = 3$, (Fig. 7). Accordingly, gated Ca^{2+} entry appears to be necessary, if not essential, for P2X receptor agonist inhibition of hormone-stimulated Mg^{2+} uptake. On balance, these observations indicate that ATP

Fig. 5. P2Y purinoceptor agonists do not inhibit Mg^{2+} uptake in MDCT cells. The cells were pretreated with indomethacin before study. UTP or ADP, at concentrations of 10^{-4} M, were added where indicated. Arginine vasopressin (AVP), 10^{-7} M, was added 5 min after treatment with the individual nucleotide. Mg^{2+} uptake was determined by techniques outlined in legend to Fig. 1. $d([Mg^{2+}]_i)/dt$ was measured over the first 500 s after addition of AVP and 1.5 mM $MgCl_2$. Values are means \pm SE for 4–5 cells. * $P < 0.01$, significance of control uptake rates.



affects Mg^{2+} entry through P2X purinoceptors that are associated with ionotropic responses.

Finally, as P2Y receptors are coupled to G proteins that commonly affect intracellular cAMP formation, we determined the effect of the purinoceptor agonists on cAMP. The nucleotides ATP, ADP, UTP, 2-MeS-ATP, and β,γ -Me-ATP do not stimulate intracellular cAMP formation in MDCT cells (Table 2). The nucleotides also did not alter PTH-responsive cAMP generation (Table 2). Accordingly, the P2Y purinoceptors do not appear to be coupled to $G\alpha_s$ or $G\alpha_i$ proteins involved with mediation of intracellular cAMP accumulation. Again, these results support the notion that ATP inhibits Mg^{2+} uptake through the P2X purinoceptor.

We have shown that adenosine increases Mg^{2+} uptake via A_2 receptors (12a). We also found in these studies that ATP inhibits adenosine-stimulated Mg^{2+}

entry. Accordingly, it is unlikely that degradation of extracellular ATP to ADP, AMP, and adenosine by ectonucleotidases plays a role in ATP inhibition of basal and hormone-stimulated Mg^{2+} uptake in MDCT cells.

DISCUSSION

This study shows that ATP inhibits basal and hormone-stimulated Mg^{2+} transport in MDCT cells. There are two major subtypes of ATP purinoceptors, P2X and P2Y, that have been characterized pharmacologically according to their respective rank order of responses to selected purine and pyrimidine agonists (21). More recently, these receptors have now been further divided into P2X1–7 and P2Y1–8 subtypes according to

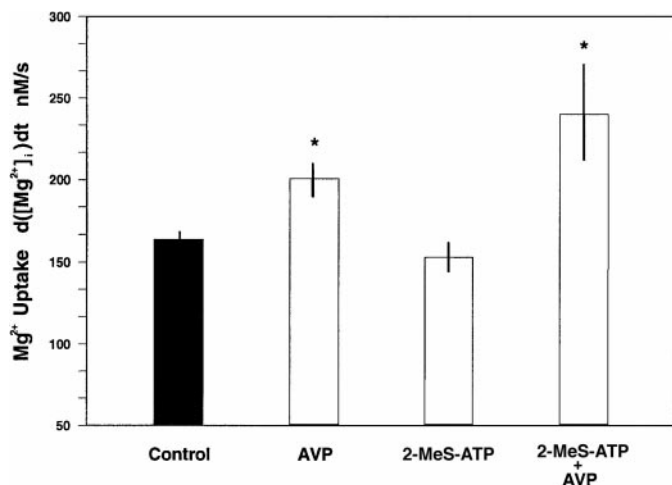


Fig. 6. The P2Y agonist 2-MeS-ATP does not inhibit AVP-mediated Mg^{2+} uptake. The more P2Y-selective agonist 2-MeS-ATP (10^{-4} M) was added where indicated \sim 5 min before AVP, 10^{-7} M. Cells were not pretreated with indomethacin in these studies. Values are means \pm SE for 4–5 cells. * $P < 0.01$, significance of control uptake rates.

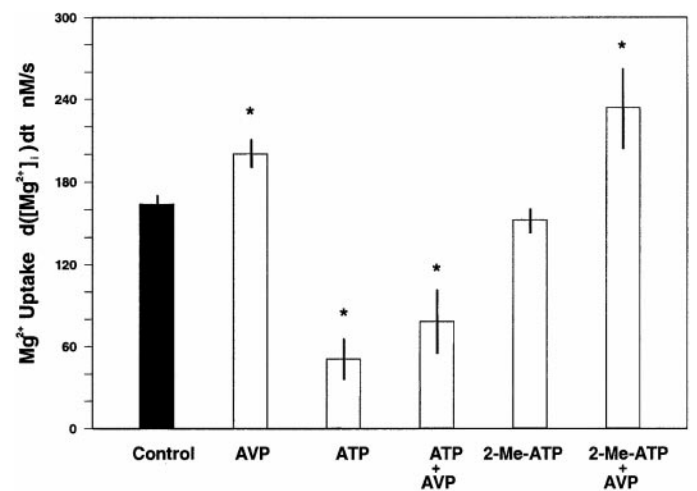


Fig. 7. P2X purinoceptor agonists inhibit hormone-mediated Mg^{2+} uptake. The more P2X-selective agonist β,γ -Me-ATP was added where indicated at concentrations of 10^{-4} M, and AVP was added at 10^{-7} M. Where indicated, extracellular Ca^{2+} was removed from the buffer solution with the addition of 0.5 mM EGTA 10 min before the addition of β,γ -Me-ATP, 10^{-4} M, and AVP, 10^{-7} M. Values are means \pm SE for 4–5 cells. * $P < 0.01$, significance of control uptake rates.

Table 2. *Purinoreceptor agonists do not alter intracellular cAMP accumulation in MDCT cells*

	Control	PTH
Control	24 ± 1(3) ⁿ	105 ± 7*(3)
ATP	25 ± 4(4)	109 ± 1†(4)
ADP	31 ± 4(4)	97 ± 6†(4)
UTP	27 ± 3(4)	103 ± 5†(4)
β,γ-Me-ATP	20 ± 5(4)	91 ± 8†(3)
2-MeS-ATP	25 ± 6(4)	134 ± 2†(3)

Values are means ± SE of cAMP accumulation (pmol·mg protein⁻¹·5 min⁻¹) with the number of separate observations in parentheses. The nucleotides, 10⁻⁴ M, were added 5 min before the addition of parathyroid hormone (PTH), 10⁻⁷ M, and cAMP was measured 5 min later. *Indicates significance, $P < 0.001$, from control values without the nucleotide and †indicates significance of nucleotide plus PTH vs. PTH alone.

their molecular identity and their intracellular signal transduction pathways (21). Biochemical and functional studies using RT-PCR and fluorescence measurements, respectively, provided evidence that both P2X and P2Y receptor families are present in MDCT cells. Our study using RT-PCR analysis showed that P2X1, P2X2, P2X3, P2X4, and P2X5 isoforms are represented in MDCT cells. We did not fully characterize the P2Y subtypes because our evidence indicates that this receptor family does not affect Mg^{2+} uptake. Nor did we attempt to identify which P2X purinoreceptor subtype inhibits Mg^{2+} entry because of the pharmacological uncertainty of identifying P2 receptors when more than one subtype is expressed in the same cell type. Agonists and antagonists show cross-reactivity, similar affinities, and different responses based on the specific cell types. Furthermore, the functional classification of P2 receptors is made even more complex by the likelihood that P2X and P2Y receptor subtypes may combine to form heteromultimeric receptors, whose functional properties are distinct from the homomultimeric receptors (21). However, the evidence that ATP acts through P2X and not P2Y purinoreceptor subtypes in MDCT cells is persuasive. The nucleotides ADP, UTP, and 2-MeS-ATP, which have a preference for the P2Y receptor, did not alter basal or hormone-stimulated Mg^{2+} uptake (Fig. 5). P2Y purinoreceptors are coupled to heterotrimeric G proteins that either stimulate or inhibit adenylate cyclase (21). The nucleotides used in this study did not alter basal cAMP concentration nor inhibit AVP receptor-mediated cAMP generation (Table 2). Accordingly, P2Y receptors are represented in MDCT cells as indicated by RT-PCR and agonist-elicited intracellular Ca^{2+} signals, but the physiological function of P2Y purinoreceptors in MDCT cells is not apparent from these studies. Conversely, the P2X receptor agonists β,γ-Me-ATP and benzoyl-benzoyl-ATP inhibited Mg^{2+} entry in a similar fashion as that observed with ATP (Fig. 7). P2X purinoreceptors are coupled to ATP-gated channels that on activation let Ca^{2+} enter the cell. Removal of extracellular Ca^{2+} blocked the rise in intracellular Ca^{2+} (Fig. 5) and prevented ATP inhibition of AVP-stimulated Mg^{2+} uptake (Fig. 7), indicating that gated channels typical of

P2X receptors are involved in mediating ATP effects rather than receptor-coupled G proteins characteristic of P2Y purinoreceptors. These findings indicate that ATP modifies Mg^{2+} uptake via P2X purinoreceptors.

ATP acting via P2X purinoreceptors plays an important role in control of epithelial transport. Filipovic et al. (10) have provided functional and molecular evidence for P2X receptors, possibly the P2X1 isoform, in LLC-PK₁ cells. McCoy et al. (17) have reported that P2X purinoreceptors that inhibit Na⁺ absorption and Cl⁻ secretion are present in a mouse IMCD cell line. Using RT-PCR, they identified two isoforms, P2X3 and P2X4 receptors, in these cells. Luo et al. (16) demonstrated P2X receptors, comprising P2X1, P2X4, and P2X7 subtypes, in luminal and basolateral membranes of pancreatic duct cells that were capable of activating Cl⁻ channels. Taylor et al. (26) surveyed the P2X isoforms expressed in a range of pulmonary- and gastrointestinal-derived epithelial cells. Their studies identified multiple isoforms that encompassed P2X1–P2X7 in various epithelial cells, with P2X6 being notably absent. Their studies suggest that a large number of P2X isoforms may mediate ATP signaling and Cl⁻ transport in epithelium disturbed in cystic fibrosis (26). In the present study, we demonstrate that P2X1–P2X5 subtypes are represented in MDCT cells, so that ATP may influence Mg^{2+} entry via any or all of these isoforms.

We have previously shown that endogenous production of prostanoids may stimulate basal Mg^{2+} entry in MDCT cells, as indomethacin, a cyclooxygenase inhibitor, diminished Mg^{2+} uptake (6). It was of interest therefore that ATP also inhibited basal Mg^{2+} entry to a similar extent as indomethacin (Fig. 2). ATP also inhibited exogenous PGE₂-stimulated uptake (6). Accordingly, we speculate that ATP may inhibit the autostimulatory prostanoid pathway. Van Baal et al. (27) also showed that ATP diminished endogenously generated prostanoids in primary rabbit cortical connecting tubule and collecting duct cells, but in their studies ATP did so via P2Y receptors. The mechanism by which ATP inhibits endogenous prostanoid release is unknown. ATP, by the P2Y purinoreceptor, has been reported to increase prostaglandin release that, in turn, enhances cAMP production in MDCK cells (19). ATP did not alter cAMP formation in MDCT cells (Table 2) so that is not evident how ATP inhibits the autostimulatory prostanoid pathway in MDCT cells.

The distal tubule reabsorbs significant amounts of Mg^{2+} and plays an important role in determining the final urinary excretion rate (20). In contrast to more proximal segments of the nephron, distal Mg^{2+} transport processes are postulated to be active and transcellular in nature (8). Hormonal control of Mg^{2+} transport in this segment provides the fine-tuning of renal conservation, contributing to whole body Mg^{2+} balance. ATP plays a physiological/pathological role in control of water in electrolyte reabsorption by the terminal segments of the nephron (13, 15, 17, 22). The present study suggests that these nucleotides may also affect Mg^{2+} transport in the distal convoluted tubule. Local

concentrations of ATP and its metabolites may be high enough to affect autocrine-paracrine function in the distal tubule (3). A number of models of cellular ATP release, metabolism, and luminal and basolateral functions have been postulated (9, 25–28). Although it is difficult to envision a role for nucleotides in the physiological regulation of renal Mg^{2+} balance, Mg^{2+} excretion, like that of other electrolytes, is dependent on the filtered load. ATP, through its actions on the afferent and efferent arterioles, decreases glomerular filtration rate and filtered Mg^{2+} (2). Accordingly, it may be appropriate to have reduced distal Mg^{2+} reabsorption in this condition to balance diminished filtered load. Whatever the rationale for nucleotide actions, it appears that ATP-mediated inhibition of $NaCl$ and Ca^{2+} reabsorption is associated with similar changes in Mg^{2+} transport in the distal nephron.

We thank Dr. Peter A. Friedman for providing the MDCK cell line. Dr. Hyung Sub Kang is a Postdoctoral Fellow of the Korean Science and Engineering Foundation.

This work was supported by a research grant from the Canadian Institutes of Health Research (MT-5793).

REFERENCES

1. **Abbraccio MP and Burnstock G.** Purinoceptors: are there families of P2X and P2Y purinoceptors? *Pharmacol Ther* 64: 445–475, 1994.
2. **Bailey MA, Imbert-Teboul M, Turner C, Marsy S, Srail K, Burnstock G, and Unwin RJ.** Axial distribution and characterization of basolateral P2Y receptors along the rat renal tubule. *Kidney Int* 58: 1891–1901, 2000.
3. **Chan CM, Unwin RJ, and Burnstock G.** Potential functional roles of extracellular ATP in kidney and urinary tract. *Exp Nephrol* 6: 200–207, 1998.
4. **Cuffe JE, Bielfeld-Ackermann A, Thomas J, Leipziger J, and Korbmacher C.** ATP stimulates Cl^- secretion and reduces amiloride-sensitive Na^+ absorption in M-1 cortical collecting duct cells. *J Physiol (Lond)* 524: 77–90, 2000.
5. **Dai L-J, Bapty BW, Ritchie G, and Quamme GA.** Glucagon and arginine vasopressin stimulate Mg^{2+} uptake in mouse distal convoluted tubule cells. *Am J Physiol Renal Physiol* 274: F328–F335, 1998.
6. **Dai L-J, Bapty BW, Ritchie G, and Quamme GA.** PGE₂ stimulates Mg^{2+} uptake in mouse distal convoluted tubule cells. *Am J Physiol Renal Physiol* 275: F833–F839, 1998.
7. **Dai L-J, Ritchie G, Bapty BW, Kerstan D, and Quamme GA.** Insulin stimulates Mg^{2+} uptake in mouse distal convoluted tubule cells. *Am J Physiol Renal Physiol* 277: F907–F913, 1999.
8. **Dai L-J, Ritchie G, Kerstan D, Kang HS, Cole DEC, and Quamme GA.** Mg^{2+} transport in the distal nephron plays an important role in determining normal and abnormal renal Mg^{2+} balance. *Physiol Rev* 81: 51–84, 2001.
9. **Deetjen P, Thomas J, Lehrmann H, Kim SJ, and Leipziger J.** The luminal P2Y receptor in the isolated perfused mouse cortical collecting duct. *J Am Soc Nephrol* 11: 1798–1806, 2000.
10. **Filipovic DM, Adebajo OA, Zaidi M, and Reeves WB.** Functional and molecular evidence for P2X receptors in LLC-PK₁ cells. *Am J Physiol Renal Physiol* 274: F1070–F1077, 1998.
11. **Friedman PA and Gesek FA.** Calcium transport in renal epithelial cells. *Am J Physiol Renal Fluid Electrolyte Physiol* 264: F181–F198, 1993.
12. **Friedrich F, Weiss H, Paulmichl M, Woll E, Waldegger S, and Lang F.** Further analysis of ATP-mediated activation of K^+ channels in renal epitheloid Madin Darby canine kidney (MDCK) cells. *Pflügers Arch* 418: 551–555, 1991.
- 12a. **Kang HS, Kerstan D, Dai L-J, Ritchie G, and Quamme GA.** Adenosine modulates Mg^{2+} uptake in distal convoluted tubule cells via A₁ and A₂ purinoceptors. *Am J Physiol Renal Physiol* In press.
13. **Kishore BK, Lin CL, and Knepper MA.** Extracellular nucleotide receptor inhibits AVP-stimulated water permeability in inner medullary collecting duct. *Am J Physiol Renal Fluid Electrolyte Physiol* 269: F863–F869, 1995.
14. **Korngruen A, Ma W, Priel Z, and Silverberg SD.** Extracellular ATP directly gates a cation-selective channel in rabbit airway ciliated epithelial cells. *J Physiol (Lond)* 508: 703–720, 1998.
15. **Koster HPG, Hartog A, van Os CH, and Bindels RJM.** Inhibition of Na^+ and Ca^{2+} reabsorption by P_{2u} purinoceptors requires PKC but not Ca^{2+} signaling. *Am J Physiol Renal Fluid Electrolyte Physiol* 270: F53–F60, 1996.
16. **Luo X, Zheng W, Yan M, Lee MG, and Muallem S.** Multiple functional P2x and P2y receptors in the luminal and basolateral membranes of pancreatic duct cells. *Am J Physiol Cell Physiol* 277: C205–C215, 1999.
17. **McCoy DE, Taylor AL, Kudlow BA, Karlson K, Slattery MJ, Schwiebert LM, Schwiebert EM, and Stanton BA.** Nucleotides regulate $NaCl$ transport in mIMCD-K2 cells via P2X and P2Y purinergic receptors. *Am J Physiol Renal Physiol* 277: F552–F559, 1999.
18. **Middleton JP, Mangel AW, Basavappa S, and Fitz JG.** Nucleotide receptors regulate membrane ion transport in renal epithelial cells. *Am J Physiol Renal Fluid Electrolyte Physiol* 264: F867–F873, 1993.
19. **Post SR, Rump LC, Zambon A, Hughes RJ, Buda MD, Jacobson JP, Kao CC, and Insel PA.** ATP activates cAMP production via multiple purinergic receptors in MDCK-D1 epithelial cells: blockade of an autocrine/paracrine pathway to define receptor preference of an agonist. *J Biol Chem* 273: 23093–23097, 1998.
20. **Quamme GA.** Renal Mg^{2+} handling: new insights in understanding old problems. *Kidney Int* 52: 1180–1195, 1997.
21. **Ralevic V and Burnstock G.** Receptors for purines and pyrimidines. *Pharmacol Rev* 50: 413–492, 1998.
22. **Rouse D, Leite M, and Suki WN.** ATP inhibits the hydrotropic effect of AVP in rabbit CCT: evidence for a nucleotide P_{2u} receptor. *Am J Physiol Renal Fluid Electrolyte Physiol* 267: F289–F295, 1994.
23. **Simmons NL.** Stimulation of Cl^- secretion by exogenous ATP in cultured MDCK epithelial monolayers. *Biochim Biophys Acta* 646: 231–242, 1981.
24. **Takeda M, Kobayashi M, and Endou H.** Establishment of a mouse clonal early proximal tubule cell line and outer medullary collecting duct cells expressing P2 purinoceptors. *Biochem Mol Biol Int* 44: 657–664, 1998.
25. **Taylor AL, Kudlow BA, Marrs KL, Gruenert DC, Guggino WB, and Schwiebert EM.** Bioluminescence detection of ATP release mechanisms in epithelia. *Am J Physiol Cell Physiol* 275: C1391–C1406, 1998.
26. **Taylor AL, Schwiebert LM, Smith JJ, King C, Jones JR, Sorscher EJ, and Schwiebert EM.** Epithelial P2X purinergic receptor channel expression and function. *J Clin Invest* 104: 875–884, 1999.
27. **Van Baal J, Hoenderop JGJ, Groenendijk M, van Os CH, Bindels RJM, and Willems PHGM.** Hormone-stimulated Ca^{2+} transport in rabbit kidney: multiple sites of inhibition by exogenous ATP. *Am J Physiol Renal Physiol* 277: F899–F906, 1999.
28. **Wilson PD, Hovator JS, Casey CC, Fortenberry JA, and Schwiebert EM.** ATP release mechanisms in primary cultures of epithelia derived from the cysts of polycystic kidneys. *J Am Soc Nephrol* 10: 218–229, 1999.